Dynamics of the ITCZ–Equatorial Cold Tongue Complex and Causes of the Latitudinal Climate Asymmetry*

BIN WANG

Department of Meteorology, University of Hawaii, Honolulu, Hawaii

YUQING WANG

Bureau of Meteorology Research Centre, Melbourne, Victoria, Australia

(Manuscript received 20 November 1997, in final form 22 July 1998)

ABSTRACT

A coupled atmosphere–ocean–coastline model driven by solar radiation is advanced to understand the essential physics determining the annual cycle of the intertropical convergence zone (ITCZ)–equatorial cold tongue (ECT) complex and associated latitudinal climate asymmetry. With a thermocline depth similar to that of the western Pacific, the aquaplanet climate is latitudinal *symmetric and stable*. The presence of an oceanic *eastern boundary* supports an *east–west* asymmetric climate and an ECT due to unstable air–sea interaction and counter stabilization provided by zonal differential surface buoyancy flux. Formation of *latitudinal climate asymmetry* requires the presence of the ECT.

The *antisymmetric solar forcing due to annual variation of the solar declination angle* can convert a *stable* latitudinal symmetric climate into *a bistable-state latitudinal asymmetric climate* by changing trade winds, which in turn control annual variations of the ECT. The ECT then interacts with ITCZ, providing a *self-maintenance mechanism* for ITCZ to linger in one hemisphere, either the northern or southern, depending on initial conditions. The establishment of the *bistable-state asymmetry* requires a delicate balance between counter effects of the antisymmetric solar forcing and self-maintenance. Two factors are critical for the latter: (i) The annual variation of ECT follows the SST of the ITCZ-free hemisphere and the meridional SST gradients between the ECT and ITCZ sustain moisture convergence, which prolongs residence of the ITCZ in summer hemisphere. (ii) The latent heat released in the ITCZ produces remarkable asymmetry in Hadley circulation and trades between the two hemispheres, and the stronger evaporation cooling in the ITCZ-free hemisphere delays and weakens the warming and convection development in that hemisphere.

The *annual cycle of insolation due to the earth–sun distance variation* may convert the bistable-state asymmetry into a *preferred latitudinal asymmetric climate.* The earth's present orbit (with a minimum distance in December solstices) favors ITCZ staying north of the equator by compelling the ECT into a delayed in-phase variation with the Southern Hemisphere SST. With annual-mean solar forcing a tilted eastern boundary can support a weak preferred latitudinal asymmetry. Inclusion of the *annual variation of insolation* can dramatically amplify the asymmetry in the mean climate through the self-maintenance mechanism.

1. Introduction

The ITCZ characterized by a narrow band of boundary layer convergence and deep convective clouds constitutes an ascending branch of the Hadley circulation and plays a central role in maintaining tropical circulation, transporting heat and momentum poleward, and balancing water and energy in the troposphere. Over the eastern-central Pacific and Atlantic Oceans, the ITCZ is mostly in the Northern Hemisphere (NH) and exhibits a distinct annual cycle in its strength and latitudinal locations.

Meteorological explanations of why the ITCZ tends to form away from the equator were primarily based on atmospheric *internal dynamics*, which emphasize the role of the planetary boundary layer processes in organizing deep convection. Charney (1971) argued that the preferred latitude for ITCZ is determined by a balance between the Ekman pumping efficiency, which increases with latitude and the moisture supply, which in turn decreases with latitude. Holton et al. (1971) viewed ITCZ as resulted from zonally propagating synoptic disturbances, which maximize boundary layer convergence at a critical latitude (around 8°) where the frequency of

* School of Ocean and Earth Science and Technology Publication Number 4768.

Corresponding author address: Dr. Bin Wang, Department of Meteorology, University of Hawaii at Manoa, 2525 Correa Rd, Honolulu, HI 96822.
E-mail: bwang@soest.hawaii.edu.

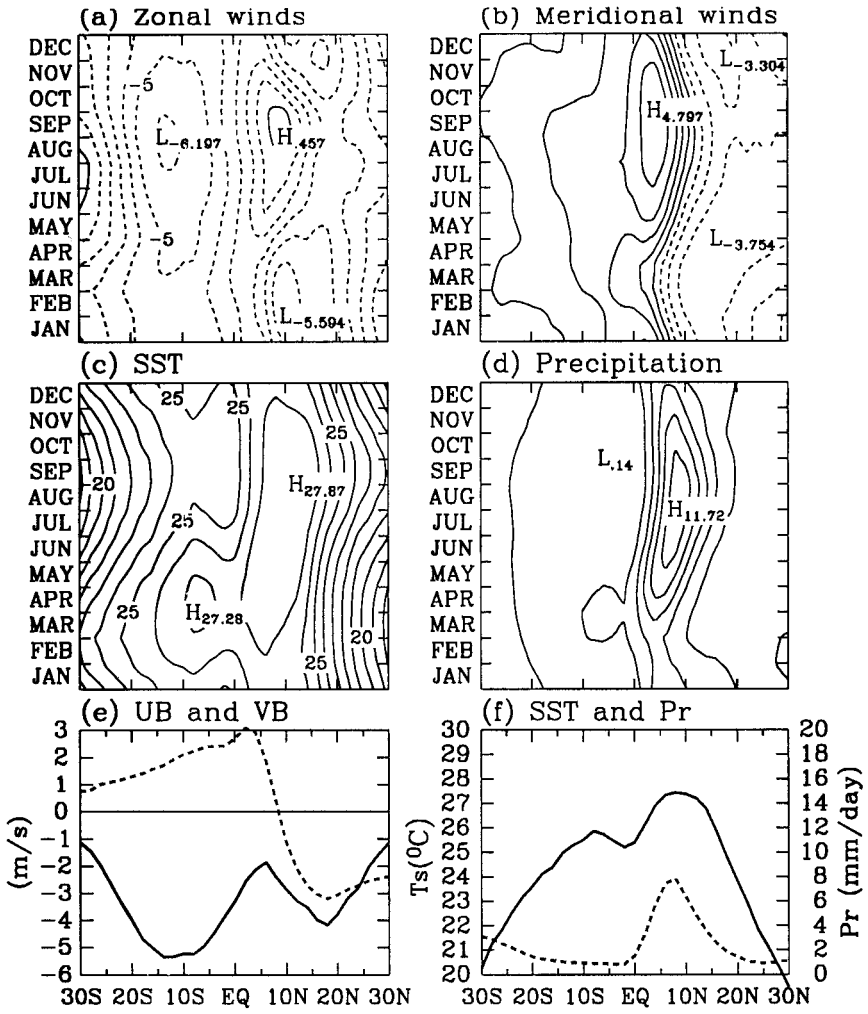

FIG. 1. Observed climatological monthly mean (a) surface zonal and (b) meridional (c) winds (m s^{-1}), SST (°C), and (d) rainfall (mm day^{-1}). Observed annual-mean surface zonal (solid) and meridional (dashed) winds (e), SST (solid), and rainfall rate (dashed) (f) over the eastern Pacific Ocean zonally averaged from 150°W to the American coast. The surface winds and SST are derived from COADS climatology (Sadler et al. 1987). The rainfall data are obtained from Xie and Arkin (1996).

the transients equals the Coriolis parameter. Waliser and Somerville (1994) demonstrated that a positive feedback between the midtropospheric latent heating and low-level convergence may enhance organization of convection at latitudes about 4°–12° lat without invoking the two mechanisms mentioned above. Wang and Li (1994) derived a solution for the Ekman pumping in an equatorial beta-plane boundary layer, which shows that convergence is associated with low pressure and eastward and poleward winds. Large-scale equatorial westerlies are often associated with off-equatorial lows and poleward winds, which tend to repel convection away from the equator. While atmospheric internal dynamic processes may coerce ITCZ away from the equator, they failed to explain why the ITCZ favors a particular hemisphere, or the latitudinal climate asymmetry.

Figures 1 and 2 show climatological mean and annual cycle of the surface winds, precipitation, and SST zonally averaged for the eastern (150°W to the American coast) and the western (110°E to the date line) Pacific, respectively. The annual-mean rainfall and SST are nearly symmetric about the equator in the western Pacific, whereas they are highly asymmetric in the eastern Pacific. The annual cycles also differ remarkably between the eastern and western Pacific. These contrasting features are found in a larger longitudinal extent between the Eastern and Western Hemispheres (Mitchell and Wallace 1992; Waliser and Somerville 1994). There is, however, one notable feature common to both the western and eastern Pacific, that is, the surface zonal and meridional winds are always significantly stronger in the winter hemisphere. Another notable feature is that

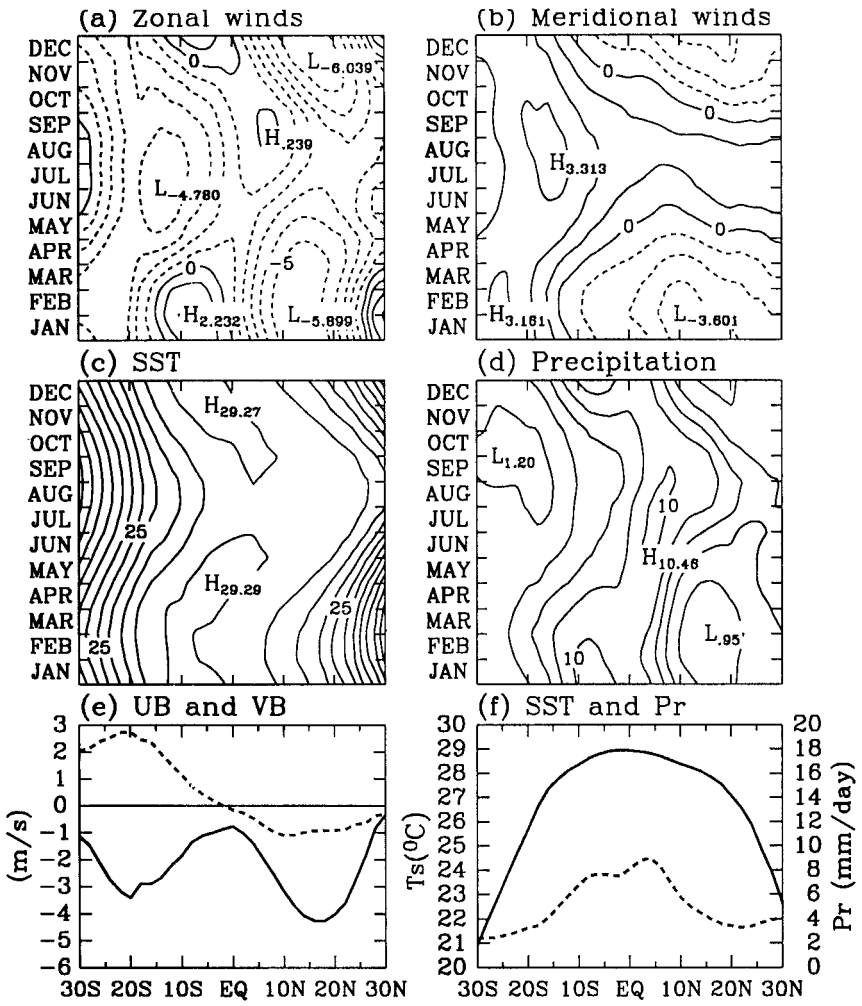

FIG. 2. Same as in Fig. 1 except for the western Pacific Ocean zonally averaged from 110°E to the date line.

the annual march of ITCZ is in tandem with the underlying SST variation, both at the equator and at the northern subtropics. The coupled variation of the ITCZ and equatorial cold tongue (ECT) was documented by Murakami et al. (1992) and Mitchell and Wallace (1992). These studies suggest that the ITCZ in the Western Hemisphere oceans is not determined by atmospheric internal dynamics alone. Both the ITCZ and the ECT belong to the same coupled climate system over the eastern Pacific and Atlantic Oceans.

Philander et al. (1996) attributed the latitudinal climate asymmetry to two sets of factors: interactions between ocean and atmosphere that are capable of converting symmetry into asymmetry, and the geometries of the continents that determine in which longitudes the interactions are effective and in which hemisphere the warmest water and the ITCZ are located. Chang and Philander showed that the positive meridional wind–SST feedback can yield an *unstable* antisymmetric mode that is relevant to explanation of the north–south asymmetry in SST. In coupled ocean–atmosphere general circulation models, however, Philander et al. (1996) found that this unstable antisymmetric mode failed to generate appreciable climate asymmetry. Instead, they discovered the importance of the positive feedback between low-level stratus clouds and SST via changing shortwave radiation in keeping ITCZ mostly north of the equator. In their experiments, the parameterized stratus clouds were overdeveloped compared with observations, thus the role of stratus–SST feedback may be somewhat exaggerated. Nevertheless, the positive stratus–SST feedback was elucidated by the linear stability analysis of Li (1997), and the efficiency of Peruvian stratus clouds in lowering SST in the Southern Hemisphere (SH) and equatorial regions were confirmed by Ma et al. (1996) using observed stratus clouds embedded in their coupled models.

The current explanation of the latitudinal climate asymmetry has been based on unstable air–sea interaction but ignored the potential roles of the annual var-

iation of insolation. Whereas the air–sea interaction is one of the major players in the annual cycle of the ECT, it does not explain why the equatorial SST variation should have an annual period. Solar radiation forcing must control the period of the SST variation at the equator even though not in a direct manner. The question is how this happens. Wang (1994) hypothesized that *the antisymmetric insolation forcing can regulate the ECT indirectly through changing the intensity of the trade winds.* He showed that the decline of the austral winter trades in the SH initiates coastal warming off Peru, which then ''propagates'' equatorward and westward through air–sea interaction and causes annual weakening of the ECT. Liu and Xie's (1994) theoretical analysis demonstrates how an extratropical annual forcing along the coast of South America can effectively influence the ECT through equatorward and westward propagation of the coupled disturbances by wind-evaporation–entrainment feedback (also see Xie 1996). Wang's hypothesis was based on the finding that the annual variation of eastern-central Pacific climate is alternatively dominated by an antisymmetric (w.r.t. the equator) component peaking in February and August and a quasi-symmetric component peaking in May and November, both having a period of 1 yr (see also Nigam and Chao 1996; Chang 1996). The former is forced by differential insolation between the NH and the Southern Hemisphere (SH) whereas the latter originates from atmosphere–ocean interaction. The antisymmetric component behaves like a monsoon with cross-equatorial flow reversing its direction annually. It was referred to as an ''invisible'' monsoon because its amplitude is small compared with the mean trade winds so that the invisible monsoon reflects the annual variations of the strength of the trade winds. In the present study we will refer to this antisymmetric component of the annual cycle in the eastern Pacific as invisible monsoon.

We believe that the formation of the latitudinally asymmetric mean climate and the annual variation of the ITCZ–ECT complex are interactive. Failure to consider the feedback of the annual variation to the mean climate may lead to an incomplete or inadequate physical explanation of the mean climate. In the present paper, we will explore the cause of the latitudinal mean climate asymmetry and the annual variation of the ITCZ–ECT complex using a consolidated theoretical framework. Section 2 describes the theoretical model. To understand the role of the continental boundary, we start with examination of an aquaplanet climate in section 3, which is relevant to understanding the annual cycle in the western Pacific. This forced axially symmetric equilibrium state is stable to perturbations antisymmetric about the equator, while unstable to an easterly perturbation *in the presence of an eastern ocean boundary.* Sections 4 and 5 discuss causes of the longitudinal and latitudinal climate asymmetries in the eastern Pacific and Atlantic Oceans. In section 6 we further explore causes of the preferred latitudinal asymmetry of the present climate. The physical processes that are responsible for the climate asymmetry and the annual cycle of ITCZ–ECT complex are summarized and discussed in the last section.

2. The two-dimensional climate model

We consider the annual variation of the *ITCZ–ECT complex* as a response of the coupled atmosphere–ocean–coastline system to solar radiation forcing. In this section, we put forward a quasi-two-dimensional (meridional-vertical) model to describe such a forced climate system in order to elucidate essential physical processes determining the annual cycle of the ITCZ–ECT and the associated latitudinal climate asymmetry.

a. The coupled atmosphere–ocean–coastline model

The ITCZ convergence and direct ocean influence are primarily confined to the atmospheric boundary layer. But the condensational heating released in the free troposphere actively interacts with the boundary layer flows. Therefore a simplest atmospheric model suitable for study of ITCZ should include both the boundary layer and the lowest vertical mode of the free-atmospheric circulation. For this reason, the two-and-a-half layer tropical climate model developed by Wang and Li (1993) is adopted as the atmospheric component of the coupled model. Detailed formulation of the zonal-mean atmospheric model is presented in the appendix.

The ocean model is used to model SST variation. The mixed layer thermodynamics is thus an essential element. The upper-ocean dynamics is also needed when coastal effects are considered. A two-dimensional version of Zebiak and Cane's (1987) model meets our needs. The detailed formulation of the zonal-mean ocean model is given in the appendix.

The zonal averages were applied to a finite longitudinal domain. The effects of an ocean eastern boundary will be discussed in detail in section 4. The possible east–west difference in SST and associated zonal winds due to the presence of a continental boundary will be included in the ocean dynamics and thermodynamics. Major parameters appearing in the coupled model equations and the corresponding values used in the present study are listed in Table 1.

b. Solar radiation forcing

Observed downward shortwave radiation flux on the surface under clear sky, F_0, is displayed in Fig. 3a, which was computed based on the monthly mean values compiled by Budyko and Miller (1974). To facilitate physical interpretation, it is advantageous to express F_0 as a sum of an annual mean F_m, and a symmetric (F_s) and an antisymmetric (F_a) (with respect to the equator) component of the annual variation:

TABLE 1. Parameters and their values used in the coupled model.

Symbol	Parameter	Value
A	SST forcing coefficient	8 m^2 s^{-2} K^{-1}
E	Rayleigh damping coefficient in the boundary layer	1 day^{-1}
ϵ_a	Rayleigh friction coefficient in the free atmosphere	1/2 day^{-1}
C_a	Atmospheric gravity wave speed of the first-baroclinic mode	50 m s^{-1}
d	Nondimensional depth of the boundary layer	0.25
μ	Newtonian cooling coefficient in free atmosphere	1 day^{-1}
r	Ratio of the equilibrium temperature at p_2 to SST	0.7
C_D	Drag coefficient	1.3×10^{-3}
C_E	Moisture transfer coefficient	1.6×10^{-3}
α	Longwave radiational cooling coefficient	1.8 W m^{-2} K^{-1}
b	Condensational efficiency coefficient	0.7
H_1	Depth of the ocean mixed layer	30 m
H	Mean depth of the thermocline	150 m
DT_z	Temperature difference across the mixed layer base	1.7 K
g'	Reduced gravity in the upper ocean	5.6×10^{-2} m s^{-2}
ϵ_o	Rayleigh frictional coefficient in the upper ocean	1 (100 day^{-1})$^{-1}$
r_s	Viscosity coefficient in ocean Ekman layer	1 day^{-1}
κ	Ocean diffusion coefficient	10^{-3} m^2 s^{-1}

$$F_0 = F_m + F_s + F_a, \tag{2.1}$$

$$F_m = F_{00}e^{-(y/y_m)^2}, \tag{2.1a}$$

$$F_s = F_m\left[0.042\cos\frac{2\pi}{\tau}(t+8) + 0.04\cos\frac{4\pi}{\tau}(t-82)\right], \tag{2.1b}$$

$$F_a = 0.98F_{00}\left(\frac{y}{y_m}\right)\cos\frac{2\pi}{\tau}(t-172), \tag{2.1c}$$

where $\tau = 365$ days, $F_{00} = 320$ W m^{-2} denotes the annual-mean shortwave flux under clear sky at the equator, *and* $y_m = 9900$ km measures an *e*-folding scale for the decrease of annual-mean insolation, F_m, with latitude, which is small within 30° lat: the shortwave flux at 30° lat is only about 8% less than that at the equator.

The annual variation is dominated by the antisymmetric component (F_a), which measures the insolation contrast between the NH and the SH and is caused by the annual variation in the solar declination angle (Fig. 3d). The minor symmetric component of annual variation (F_s) (Fig. 3c) includes a semiannual cycle in solar declination (maximized on the equator) due to the change in declination angle and an annual cycle due to changes in the sun–earth distance (maximized on the northern winter solstice when the earth is closest to the sun). At the equator, F_s is dominant, because F_a vanishes. At about 4° lat, the two components have the same magnitude. Therefore, the variations in the symmetric component are important only in the oceanic equatorial waveguide. The antisymmetric component has a much larger amplitude in the subtropics (102 W m^{-2} at 30° lat). As will be demonstrated, the prominent annual cycle of the solar radiation in the subtropics (the antisymmetric component of insolation) has a considerable control on the tropical climate. Even at the equator where F_s dominates, the antisymmetric component has its consequential impact in an indirect manner. The sum of F_m, F_s, and F_a shown in Fig. 3b is an excellent approximation to the observed value (the maximum difference is less than 8 W m^{-2}).

3. The axially symmetric climate on an aquaplanet

Consider first an aquaplanet and neglect land effects. In this case, the upper-ocean dynamics do not play a significant role in annual variation of SST if the thermocline is as deep as in the western Pacific. The mixed layer meridional currents can be well approximated by Ekman flow. Thus, the ocean can be simply described by the Ekman dynamics, Eq. (A15), and the mixed layer thermodynamic equation, Eq. (A9) with $\Delta T_x = 0$.

To focus on the role of annual variation of solar forcing, we intentionally specify an axially symmetric distribution of cloud amount. Both the deep convection and stratus clouds would affect the downward radiation flux to the ocean (thus SST) and be influenced by SST. The interaction is complicated and we defer this complexity to future study. With a symmetric distribution of cloudiness similar to that observed in the western Pacific:

$$C = \begin{cases} 0.53, & |\phi| \le 20°, \\ 0.53 + 0.1(|\phi| - 20)/10, & |\phi| > 20°, \end{cases} \tag{3.1}$$

the coupled model yields *an axially symmetric aquaplanet climate*: the annual-mean SST, surface zonal winds, and rainfalls are all nearly symmetric about the equator (Figs. 4e,f).

The resultant steady annual cycles of rainfall, boundary layer winds, and SST (Figs. 4a–d) bear close similarities to the observed western Pacific climate (Fig. 2). Discrepancies are seen in the phases of zonal wind and rainfall and the amplitude of the equatorial zonal wind.

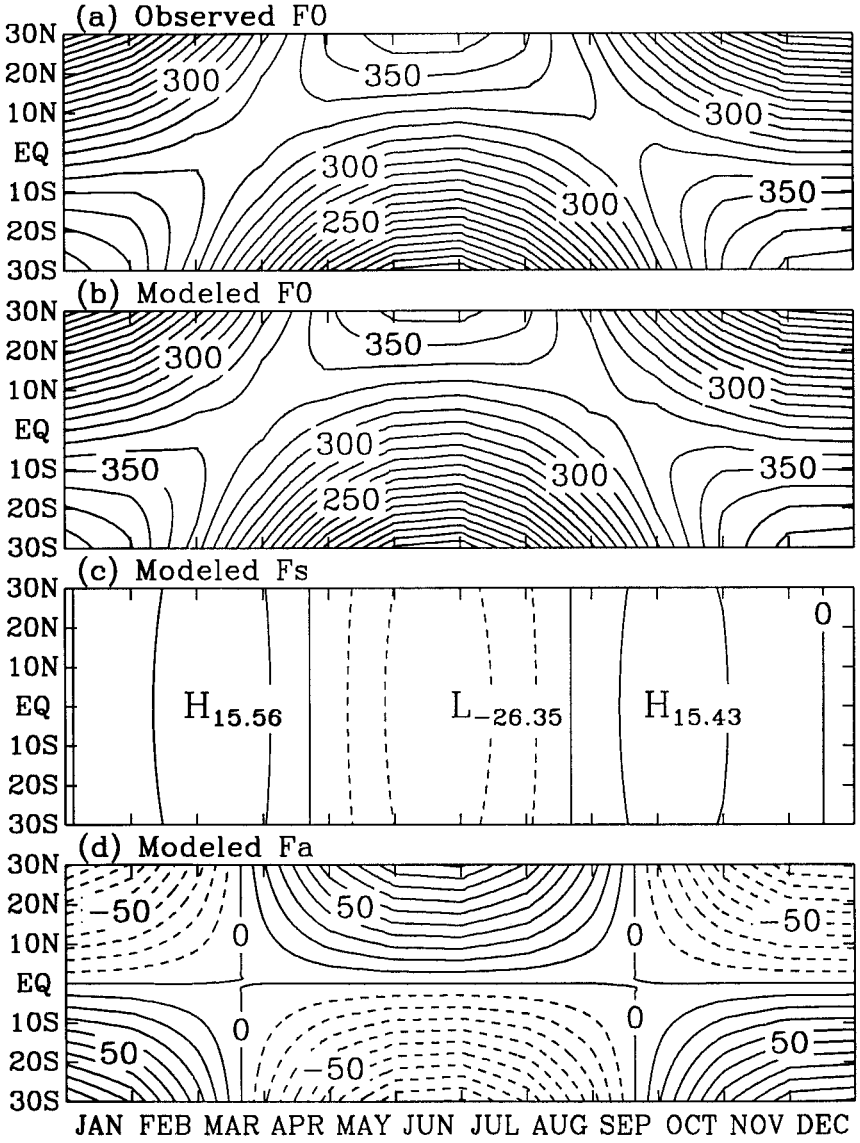

FIG. 3. (a) The observed net shortwave radiation flux (W m^{-2}) at the surface under clear sky (adopted from Budyko and Miller 1974). (b) The same quantity as in (a) except that it is computed from analytical approximation [Eq. (2.1)]. (c) and (d) Respectively, the equatorial symmetric and antisymmetric components of the annual variation in the shortwave radiation flux.

These discrepancies are primarily due to the land influence on the observed annual cycle in the western Pacific. The maximum rainfall and convergence zone migrates following the maximum SST, which lags local maximum insolation by about 2–3 months. Note that, the surface winds in the winter hemisphere are much stronger than those in the summer hemisphere, indicating a pronounced asymmetry in Hadley circulation with winter circulation amplifying greatly while the summer cell becomes very weak. This is consistent with observations and the theory of Lindzen and Hou (1988), who found that a moving peak heating even 2° off the equator leads to a remarkable asymmetry in the Hadley circulation. Another notable feature is the rapid transition between the summer and winter. Even though the seasonal march of solar forcing is a smoothed sinusoidal variation, the atmospheric circulation experiences much more abrupt changes during the transitional seasons. This suggests that the abrupt poleward shift of ITCZ during spring observed in the eastern hemisphere monsoon regions may originate from atmospheric internal dynamics.

With annual-mean solar forcing the coupled system reaches a steady symmetric climate. Initial asymmetric perturbations in SST and winds were applied to the steady symmetric climate. This coupled steady state is stable to the imposed antisymmetric perturbations, even

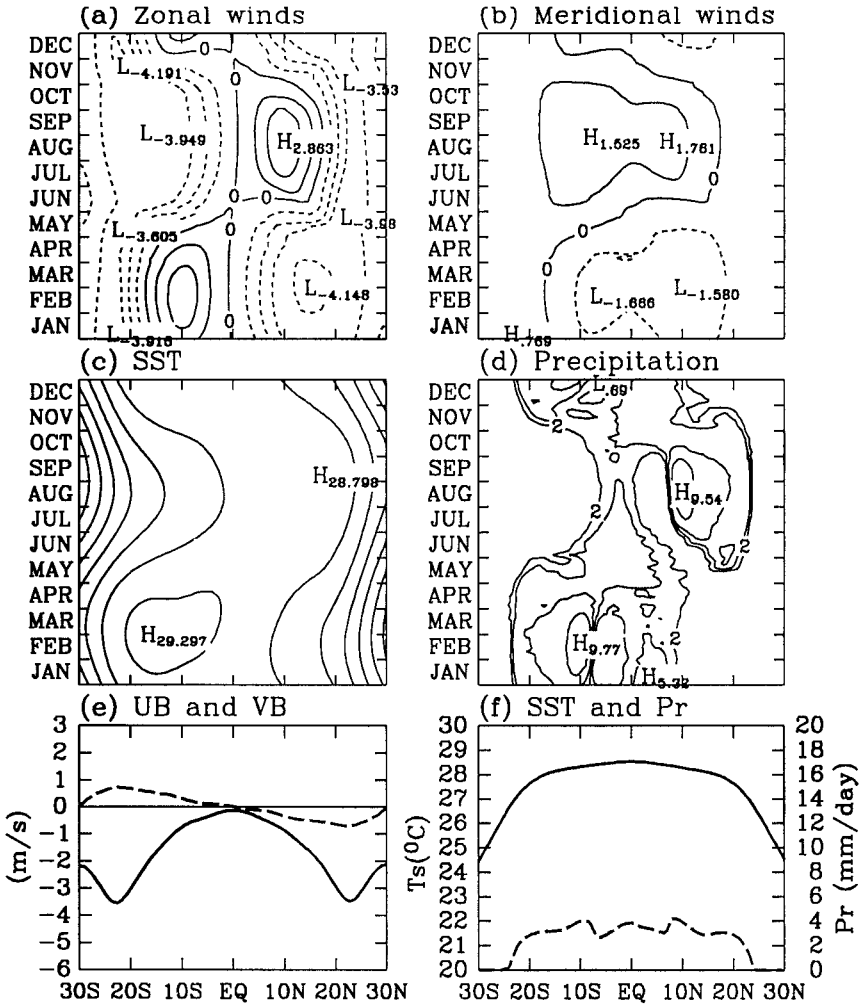

FIG. 4. As in Fig. 1 except for the model simulated aquaplanet axially symmetric climate with the present-day annual cycle of insolation forcing.

though these perturbations initially generate strong cross-equatorial flow and differential evaporation cooling between the NH and the SH. When the depth of the mean thermocline was reduced from 150 m to 100 m or 50 m, the resultant climate remains symmetric about the equator and stable to antisymmetric perturbations. The major difference lies in that the SST near the equator is lowered due to the enhanced upwelling-induced cooling and the rainfall tends to be concentrated in off-equatorial zones (more evident double ITCZ). The atmosphere–ocean interaction, such as meridional wind–SST gradient feedback (Chang and Philander 1994) or wind–evaporation feedback (Xie and Philander 1994), is unable to create latitudinal climate asymmetry in those cases. The former is a destabilizing mechanism but the induced instability is weak and confined to the equatorial waveguide. Its effect is overwhelmed by the effect of antisymmetric solar forcing. The wind–evaporation feedback, in fact, suppresses antisymmetric perturbation and tends to maintain an axially symmetric climate. For instance, consider an initial positive SST anomaly that is placed north of the equator where mean easterlies dominate. The SST anomaly would induce a low surface pressure (Lindzen and Nigam 1987) and an associated cyclonic wind anomaly due to the earth's rotation. The total wind speed thus decreases (increases) on the equatorward (poleward) side of the anomalous cyclone. The differential wind speed would cause warming (cooling) on the equatorward (poleward) side of the SST anomalies. The positive SST anomaly would shift toward the equatorial warmest water. The wind–evaporation feedback thus tends to eliminate the initial asymmetries in the SST field.

4. Causes of the equatorial east–west climate asymmetry

The aquaplanet symmetric climatic state is not only stable to monsoon perturbations forced by antisymmetric solar forcing but also stable to equatorial zonal wind

perturbations. The air–sea interaction in this case causes neither latitudinal nor zonal asymmetry. This, however, is not the case when land serves as an eastern ocean boundary.

In the presence of an ocean *eastern* boundary, the symmetric climatic state becomes unstable to a surface *easterly* perturbation. The instability arises from the interaction between the east–west (Walker) circulation and zonal SST gradients via equatorial upwelling as visualized by Bjerknes (1969). Surface easterlies induce equatorial upwelling and make the thermocline shoal to the east. The upwelling induces stronger cooling in the east because a shallow thermocline brings cold water closer to the mixed layer base. This results in a westward increase in SST along the equator, which induces a westward pressure gradient force that in turns enhances the easterly perturbation. This positive feedback leads to a simultaneous amplification of equatorial easterlies and zonal SST gradients. The Bjerknes (1969) hypothesis was originally advanced to explain the development of Pacific warming/cooling. It was later applied to understand the formation of the annual cycle (Horel 1982; Wang 1994) and mean climatology (Dijkstra and Neelin 1995; Jin 1996) of the equatorial Pacific SST.

The establishment of the east–west asymmetry requires a restoring mechanism to balance the effect of coupled instability. This is provided by zonally differential latent and sensible heat fluxes. The loss of latent heat increases with increasing SST provided the wind speed is invariant. Thus, the westward SST gradient must induce a higher (lower) latent heat loss in the central (eastern) Pacific, which prohibits the increase of westward SST gradients. The coupled system will reach an equilibrium due to the coupled instability being balanced by the damping provided by the zonally differential buoyancy flux.

Surface easterly *perturbations* are expected at the equator even under a symmetric insolation force and lower boundary conditions. This is due to the equatorward transport of angular momentum and the constraint of angular momentum conservation and the vertical momentum diffusion (Held and Hou 1980). The resultant surface equatorial easterlies on an aquaplanet climate, however, are rather weak (less than 1 m s^{-1}; Waliser 1997, personal communication). The unstable air–sea interaction at the equator, however, can amplify the equatorial easterlies and associated westward SST gradients, resulting in a finite-amplitude east–west asymmetry. The argument here emphasizes that the observed equatorial easterlies are largely a result of air–sea interaction.

Let us estimate the strength of the east–west asymmetry based on the argument presented earlier in this section. At an equilibrium state, the Rayleigh friction associated with the equatorial surface zonal wind, u_A, is approximately balanced by zonal SST gradient-induced pressure gradient force (Lindzen and Nigam 1987), thus,

$$Eu_A = A\frac{\partial T}{\partial x}, \tag{4.1}$$

the meaning of the symbols in (4.1) is explained in Table 1. In the upper ocean, the westward wind stress is approximately balanced by an eastward pressure gradient force associated with the thermocline tilt—the Sverdrup (1947) balance:

$$g'\frac{\partial h}{\partial x} = \frac{\rho_a C_D}{\rho_w H}|u_A|u_A. \tag{4.2}$$

The easterly induced equatorial upwelling can be solved from Ekman dynamics [Eq. (A15)], which yields (e.g., Wang and Fang 1996)

$$w = \frac{H_s(H - H_s)}{H}\nabla \cdot V_e = -\frac{(H - H_s)\beta}{r_s^2}\frac{\rho_a C_D}{\rho_w H}|u_A|u_A. \tag{4.3}$$

From (A9), the equilibrium mixed layer temperature is governed by

$$\frac{w}{H_s}\mathcal{H}(w)(T - T_e) = \frac{Q_{sw}(1 - \gamma) - Q_{lw} - Q_{lh}}{\rho_w C_w H_s}, \tag{4.4}$$

where the horizontal advection of temperature was neglected. Although zonal currents transport heat eastward, its effect is largely offset by equatorward cold advection by coastal current (e.g., Peru Current). As a result, the horizontal advection probably plays a minor role in creating east–west equatorial asymmetry. For simplicity, we neglect the zonal variations in u_A, w, and the shortwave and longwave radiation fluxes. Taking longitudinal (x) derivatives of Eq. (4.4) yields

$$w\mathcal{H}(w)\frac{\partial}{\partial x}(T - T_e) = \frac{-1}{\rho_w C_w}\frac{\partial Q_{lh}}{\partial x}. \tag{4.5}$$

To derive an analytical expression, we adopt the following approximations for the surface latent heat flux [see Eq. (2.10) in Wang and Li 1993]

$$Q_{lh} = L_c\rho_a C_E K_q|u_A|(T - 293), \tag{4.6}$$

and for the temperature difference across the mixed layer base (Battisti and Hirst 1989)

$$T - T_e = \Delta T_z - \lambda h. \tag{4.7}$$

Substituting Eqs. (4.6) and (4.7) into (4.5) leads to

$$w\mathcal{H}(w)\lambda\frac{\partial h}{\partial x} = \frac{L_c}{\rho_w C_w}\rho_a C_E K_q|u_A|\frac{\partial T}{\partial x}. \tag{4.8}$$

Obviously, a westerly perturbation induces downwelling ($w < 0$) [Eq. (4.3)], so that, from Eq. (4.8), the zonal SST gradient vanishes, implying that the forced zonally symmetric climates are stable to westerly perturbations. An easterly perturbation, however, induces equatorial upwelling, thus combining (4.8) and (4.3) leads to

$$-(H - H_S)\frac{\beta C_D}{Hr_s^2}u_A\lambda\frac{\partial h}{\partial x} = \frac{L_c}{C_w}C_E K_q\frac{\partial T}{\partial x}. \tag{4.9}$$

Use of Eqs. (4.1) and (4.2) in (4.9) yields

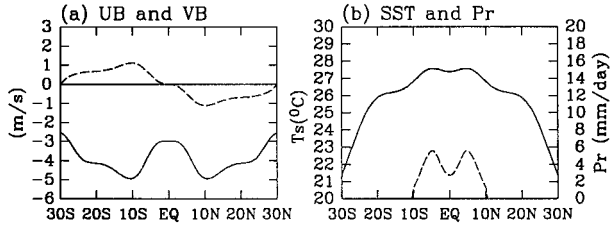

FIG. 5. (a) Steady-state response of the surface zonal (solid) and meridional (dashed) winds and (b) SST (solid) and rainfall (dashed) obtained from the coupled model simulation with annual-mean solar forcing and the equatorial east–west climate asymmetry in the presence of an eastern ocean boundary.

$$u_A = -\left[\frac{\rho_w}{\rho_a}\frac{C_E}{C_D^2}\frac{g'H^2}{(H - H_s)}\frac{Er_s^2K_q}{C_w\beta A\lambda}\right]^{1/2}. \quad (4.10)$$

Given the parameter values listed in Table 1 and $\lambda = 4 \times 10^{-2}$ K m^{-1}, the estimated equatorial zonal wind is about -3 m s^{-1}. The corresponding equatorial zonal SST gradient is about 0.5×10^{-6} K m^{-1}, corresponding to a $\Delta T_x = 4$ K between 80°W and 150°W.

Both u_A and ΔT_x are equatorially trapped due to the change of signs in the Coriolis parameter across the equator. It is reasonable to assume that they have a meridional structure of the lowest parabolic cylindrical function (Gill 1980):

$$u_A = u_A(0)e^{-(y/L_a)^2}, \quad (4.11a)$$

$$(\Delta T_x)_E = \Delta T_x(0)e^{-(y/L_o)^2}, \quad (4.11b)$$

where $u_A(0) = -3$ m s^{-1}, $\Delta T_x(0) = 4$ K, and the L_a and L_o represents, respectively, the atmospheric and oceanic equatorial Rossby radius of deformation.

In the presence of an oceanic eastern boundary, we need to incorporate the east–west asymmetry, that is, the equatorial easterlies and zonal SST difference [Eq. (4.11)] in the ocean model. The total atmospheric boundary layer winds (u_B and v_B), which drive the ocean, should be the sum of the forced zonally symmetric wind (u_b and v_b) and the zonally asymmetric wind (u_A): $(u_B, v_B) = (u_b + u_A, v_b)$. The zonal temperature advection associated with zonal SST gradient should be also included.

With annual-mean solar radiation forcing, $F_m(y)$, the steady climate is symmetric about the equator but is characterized by an equatorial cold tongue in the eastern basin due to the effect of the eastern ocean boundary (Fig. 5).

5. Causes of the latitudinal climate asymmetry

Different from the aquaplanet climate, the steady state with an ECT in the eastern basin can be unstable to *finite-amplitude* antisymmetric perturbations, as demonstrated by Li (1997) and Xie (1997). The growth rate depends on intensity of the east–west asymmetry (thus the thermocline depth) and the dissipation. The explanation of the latitudinal climate asymmetry has been primarily based on the instability of the coupled mean basic state to antisymmetric perturbations (Chang 1996; Li 1997; Xie 1997). The role of the annual cycle in insolation has been neglected. In this section we demonstrate that the antisymmetric solar forcing can convert a stable latitudinal symmetric climate to a bistable latitudinal asymmetric climate.

In our experiment, for the parameters given in Table 1, the symmetric climate forced by annual-mean insolation in the presence of the eastern boundary (or significant mean easterlies and ECT) is stable to antisymmetric perturbations, that is, the coupled antisymmetric modes are decaying. This was confirmed by time integration of the model for the symmetric climate with an imposed small-amplitude initial antisymmetric disturbance.

When this coupled system is forced by *the annual mean plus antisymmetric solar forcing*, $F_m(y) + F_a(y, t)$, the resultant annual cycle and the annual-mean climate is shown in Fig. 6. Note that all model parameters are identical to those used in Fig. 5. With the antisymmetric solar forcing included, the ITCZ tends to be biased to one hemisphere, showing evident north–south asymmetry. Depending on initial conditions, the resultant ITCZ can stay in either the NH or SH. This provides firm evidence that *the nonlinear effects of the annual variation forced by antisymmetric solar radiation can generate latitudinal asymmetry, provided the ECT or the east–west equatorial asymmetry preexists.*

The process causing the latitudinal asymmetry involves a self-maintenance mechanism arising from the interplay between the ECT and ITCZ regulated by the antisymmetric solar forcing. For convenience of discussion, suppose initially the ITCZ and corresponding high SST occur in the SH during southern solstice (late December) as the case shown in Fig. 6. When the sun moves back to the equator in the ensuing equinox season (late March), the SST in the SH (NH) subtropics reaches its maximum (minimum) due to ocean thermal inertia and the negligible role of the thermal advection. The strongest hemispheric thermal contrast renders the southern ITCZ reach maximum intensity. We note that the equatorial SST is largely controlled by the easterlies originated from the ITCZ free hemisphere (the NH in this case) through upwelling-induced vertical temperature advection. The annual cycle of the ECT has thus a phase delay compared to the annual variation of the SST in the ITCZ-free hemisphere and reaches a maximum cooling in April–May in the case discussed. Therefore, when the sun moves to the NH, the ITCZ remains in the SH, *because the ECT is coldest in April–May,* and the SST gradients south of the ECT drive the boundary layer winds southward, converging into and maintaining the southern ITCZ. This local ECT–ITCZ interaction acts against the effect of the hemispheric differential solar forcing. Thus, the feedback between the ECT and ITCZ provides a *''self-maintenance'' mechanism* that prevents ITCZ from following the maximum insolation moving back to the equator when northern

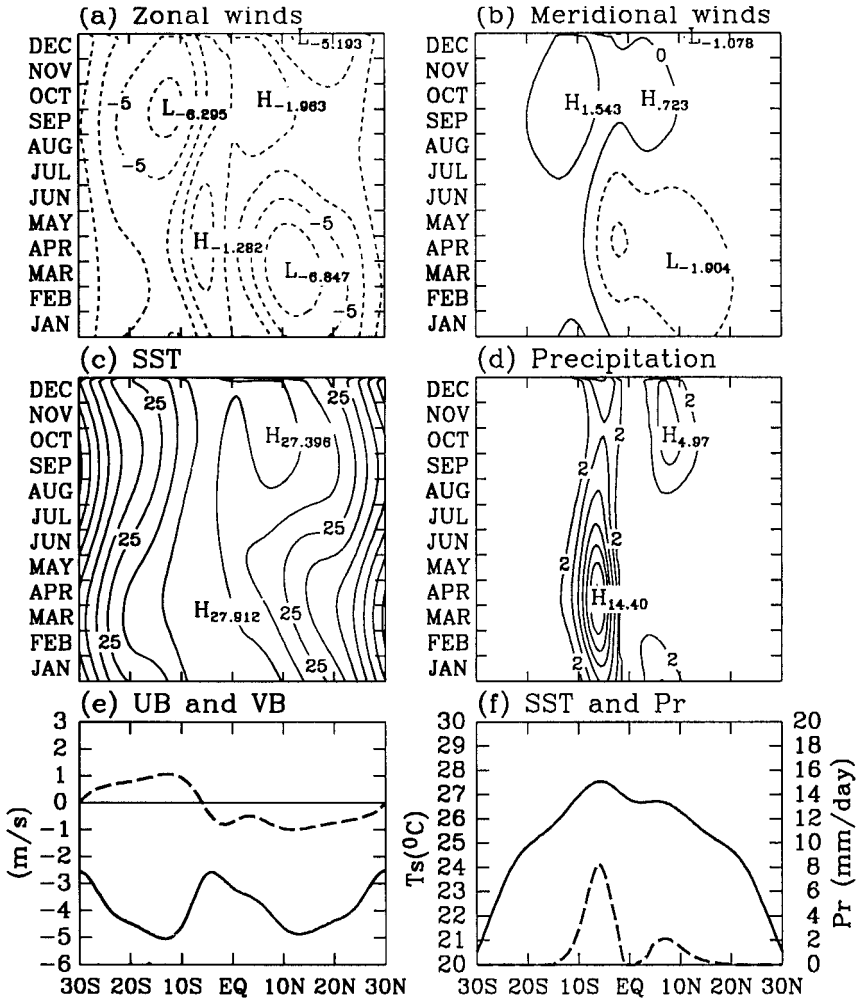

FIG. 6. The same as in Fig. 1 except for the model-simulated climate with annual mean plus antisymmetric component of insolation forcing. The equatorial zonal climate asymmetry (the equatorial easterlies and east–west SST gradients) was included in the ocean component of the coupled model. Note that the resultant latitudinal asymmetry depends on initial conditions.

solstice (late June) comes. The phase delay of the annual cycle of the ECT to that of the ITCZ-free hemisphere is important in the self-maintenance mechanism. During the following equinox season (late September), the NH SST becomes highest, a weaker northern ITCZ develops, and the southern ITCZ becomes weakest. Note that the NH SST warming and ITCZ convection in the boreal fall are weaker than their counterparts in the boreal spring. An important reason for that is the lasting evaporation cooling in the NH during the preceding two seasons when the surface winds in the NH are remarkably stronger than those in the SH. The *off-equatorial heating* released in the southern ITCZ is responsible for the remarkable asymmetric Hadley circulation and associated trade winds (Lindzen and Hou 1988; Waliser and Somerville 1994). The enhanced and prolonged evaporation cooling in the NH effectively delays and weakens the warming up of the NH water and the development of northern ITCZ. Thus the interaction between the ITCZ convection and the meridional SST gradient associated with the ECT under the regulation of antisymmetric solar forcing results in an latitudinal asymmetry in the annual-mean climate.

In the above argument, a critical point is the competition between the self-maintenance mechanism (supported by the ocean thermal inertia and the ECT–ITCZ interaction) and the efficiency of antisymmetric solar radiational forcing in overcoming ocean thermal inertia. Obviously, the maximum solar declination angle and the period of the earth's orbital rotation are two critical factors. The former determines the amplitude of the antisymmetric forcing, while the latter determine the accumulated antisymmetric heating in changing hemispheric SST contrast. Because the cloud amount is specified, which does not interact with circulation in the present model, it is unable to adequately assess the ef-

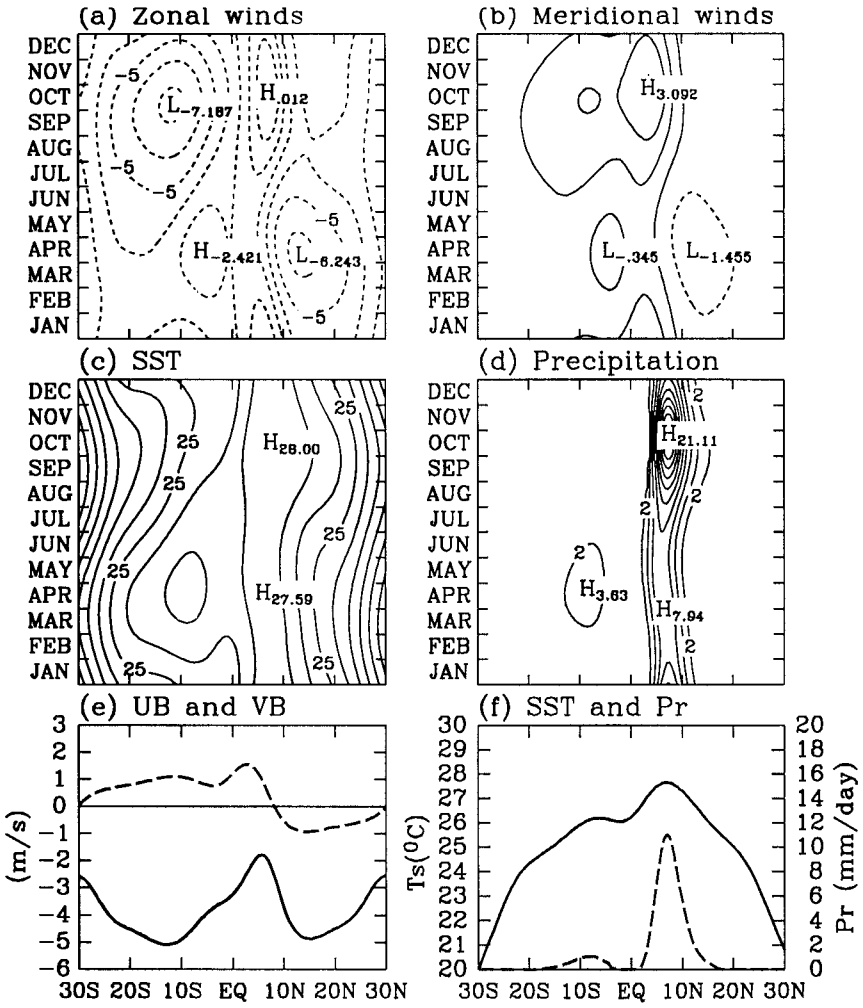

FIG. 7. The same as in Fig. 6 except that the annual variation of the symmetric insolation forcing is included. Note that the resultant latitudinal climate asymmetry does not depend on the initial condition.

fects of the changes in solar forcing. However, the coupled GCM experiment performed by Giese and Carton (1994) shows that when the length of the solar year is increased to 18 months, the ITCZ may cross the equator into the SH and the mean climate becomes latitudinally symmetric.

Although the antisymmetric forcing can cause latitudinal asymmetry in the mean climate, it does not explain why the ITCZ and warm SST are mostly in the NH. Additional factors are needed to account for this preferred latitudinal climate asymmetry.

6. Causes of the preferred latitudinal climate asymmetry

We found that one of the possible factors favoring ITCZ in the NH in the present climate is the annual variation of the sun–earth distance, which produces the annual variation of the symmetric solar forcing, $F_s(y, t)$ [Eq. (2.1b)]. When this forcing component is included, extended numerical integration of the coupled model (for 100 yr) indicates that the NH ITCZ will eventually dominate (Fig. 7). This preferred development of ITCZ in the NH does not depend on initial conditions. The reasons follow. Over the equator, the symmetric solar forcing dominates. During late December (late June), the earth–sun distance is minimum (maximum), thus the annual harmonic of the symmetric insolation at the equator reaches maximum (minimum). This tends to coerce ECT to be warmest during late March and coldest in late September; that is, the ECT is forced to vary in phase with SH SST. That favors establishment of an ITCZ north of the ECT (recall that when southern ITCZ is favored, the ECT is warmest in September and coldest in March which is in phase with the NH SST variation).

Philander et al. (1996) proposed another mechanism for the preferred latitudinal climate asymmetry in the eastern Pacific. The northwest–southeast-tilted eastern

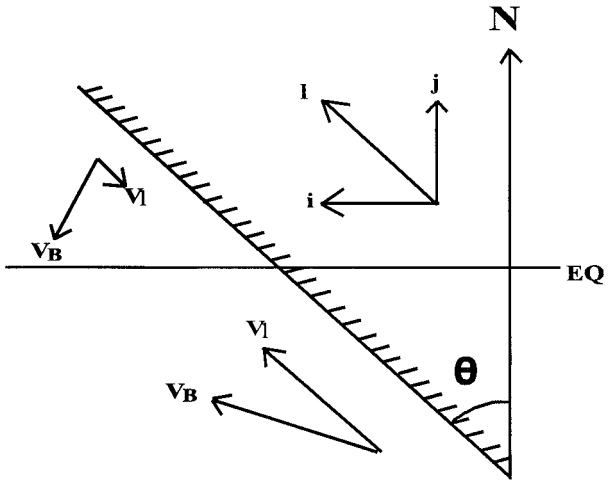

FIG. 8. Schematic diagram showing the coastline geometry and projection of the trade winds to alongshore direction considered in Eq. (6.1).

boundary favor stronger alongshore winds in the SH, which induce stronger coastal upwelling and lower SST. The latitudinal asymmetric SST along the coast then could break the symmetric climate. The coupled GCM experiments, however, show that a tilted western American coastal line can generate only a very weak latitudinal asymmetry when the coupled model is forced by *annual-mean* solar radiation. We will show that this is the case in the present two-dimensional model, however, the annual variation of insolation can dramatically amplify the latitudinal asymmetry in the mean climate.

To parameterize the effect of a tilted coastline in the quasi-two-dimensional model, consider a straight eastern boundary, which forms an angle θ with the meridian (Fig. 8). Define the orientation of the coastline by a unit vector, **l**, that has a positive northward component, thus the northward alongshore wind component can be expressed by

$$V_l = V_B \cdot l = -u_B \sin\theta + v_B \cos\theta. \qquad (6.1)$$

The coastal upwelling associated with the offshore Ekman transport depends on the sign of the Coriolis parameter and the direction and strength of the alongshore wind stress (or in a linear version, the alongshore wind speed) (O'Brien and Hurlburt 1972), thus

$$w_E = -B' f(u_B \sin\theta - v_B \cos\theta), \qquad (6.2)$$

where B' is a coefficient that can be determined emprically by fitting observation. Equation (6.2) provides a quantitative estimate of the upwelling along the coast due to the effects of the tilted coastline. The resultant asymmetry in coastal upwelling provides a source of latitudinal asymmetry in SST.

The zonal SST difference between the mid-Pacific (T_W) and the eastern boundary (T_E) induced by coastal upwelling can be approximately determined by the following thermodynamic balance between vertical temperature advection and surface evaporation cooling [Eq. (A9)]:

$$\frac{\Delta T_z}{H_s}(w_E - w_W) = \frac{L_c \rho_a C_E}{\rho_w C_w H_s} K_q |u_A|(T_E - T_w), \qquad (6.3)$$

where the zonal variations in shortwave radiation, longwave radiation, and horizontal advection of temperature have been neglected. In the midocean, there is no off-equatorial upwelling due to the absence of the ocean boundary. Use of (6.2) in (6.3) leads to

$$\Delta T_x = - fB(u_B \sin\theta - v_B \cos\theta), \qquad (6.4)$$

where B is a coefficient determined by the model parameters and B'.

Equation (6.4) depicts an eastern boundary effect on the off-equatorial east–west SST asymmetry. Due to the tilt of the coastline, the projected alongshore wind induces stronger cooling in the SH than in the NH. This results in a latitudinal asymmetric boundary forcing, which can affect zonally averaged SST and circulation by horizontal advection process. Note that the coastal upwelling at the equator vanishes due to vanishing Coriolis force, but the equatorial easterlies support east–west SST difference. Therefore, for a tilted coastline shown in Fig. 8, the total east–west SST difference includes two components: that induced by east–west asymmetry, (4.11b), and that induced by coastal asymmetry (6.4). Assume $\theta = 45°$, the estimated annual-mean east–west SST difference as a function of latitude is shown in Fig. 9b, which is qualitatively similar to observed long-term mean SST difference between the American coast and 150°W derived from the Comprehensive Ocean–Atmosphere Data Set (COADS) (Fig. 9a) except beyond about 9°N where the alongshore winds in the model induce downwelling, which does not affect coastal SST.

If the zonal temperature advection associated with the equatorial and coastal asymmetric SST distribution is included in the mixed layer thermodynamic equation, the climate under annual-mean solar radiation forcing exhibits a *moderate* asymmetry with the highest SST and maximum convection located at 5°N, although a weaker ITCZ appears also around 5°S (Fig. 10). The moderate latitudinal asymmetry obtained here is consistent with the results of Philander et al. (1996).

When *the annual variation in solar radiation* is included, the latitudinal asymmetry in an annual-mean climate is remarkably amplified (Figs. 11e,f). This indicates a profound contribution of the antisymmetric solar radiation forcing and associated transient invisible monsoon to formation of the annual-mean latitudinal asymmetric climate. The physical processes responsible for the amplification of the climate asymmetry are essentially the same as those discussed in the previous section. The interaction between the ITCZ convection and the meridional SST gradient associated with the ECT provides a primary self-maintenance mechanism to keep the ITCZ and highest SST in the NH.

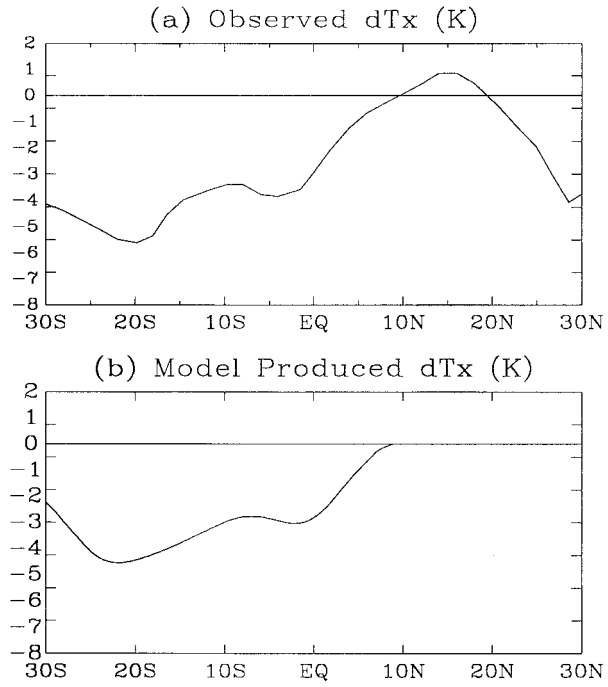

FIG. 9. (a) The observed long-term mean SST difference between the American coast and 150°W (east–west) derived from COADS. (b) The model counterpart of (a) computed from the parameterized coastal upwelling and equatorial zonal climate asymmetry.

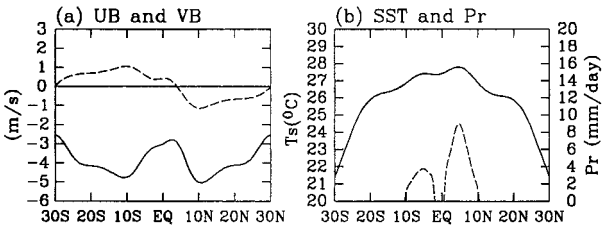

FIG. 10. The same as in Fig. 5 except that the effect of a northwest–southeast-titled eastern ocean boundary on ocean dynamics is included in the coupled model. The moderate latitudinal asymmetry results from the specified coastline asymmetry.

To assess contributions of various individual air–sea interaction processes to the formation of latitudinal climate asymmetry, we performed a series of numerical experiments with the model that produces the results in Fig. 11.

In the first experiment, the cooling induced by equatorial upwelling was removed from the mixed layer thermodynamic equation. This effectively suppresses the ECT. Without the ECT, the mean climate is symmetric (Fig. 12a). The presence of the equatorial upwelling is necessary for the latitudinal climate asymmetry even in the presence of the continental asymmetry.

When the dependence of evaporation on wind speed is removed by replacing model winds with the annual-mean winds, the simulated climate is nearly symmetric about the equator (Fig. 12b). The wind–evaporation feedback is hence one of the most important processes for the self-maintenance mechanism. This confirms the claim made by Xie and Philander (1994) and Xie (1996) based on their linear coupled model analysis with a specified equatorial upwelling. It is, however, important to recall that without the ECT or the east–west asymmetry, this mechanism alone cannot generate latitudinal asymmetry, as shown in Fig. 12a. The wind–evaporation mechanism can act to either stabilize or destabilize a symmetric climate depending on the existence of the ECT. In the presence of an ECT, the equatorward shift of a positive SST anomaly due to wind–evaporation feedback (as described earlier in section 3) would enhance the thermal contrast between the off-equatorial warm water and ECT, which would in turn enhance moisture convergence into the ITCZ and the ECT–ITCZ interaction.

The meridional SST gradient associated with the ECT in forcing surface winds plays an appreciable part. When meridional SST gradient forcing is removed from the atmospheric boundary layer momentum equation, the simulated SST difference between the ITCZ and the equator is significantly reduced (Fig. 12c). The climate asymmetry is also sensitive to changes in the efficiency of convective heating (figure not shown). These results indicate that the ITCZ–ECT interaction heavily relies on the feedback between convection-induced winds and meridional SST gradients.

If the meridional wind stress applied to the upper ocean is suppressed, the solution does not alter appreciably (Fig. 12d), indicating that the antisymmetric coupled unstable mode, which relies on meridional wind stress, is not an essential process for generation of latitudinal climate asymmetry. This conclusion agrees with Philander et al.'s (1996) assessment using coupled GCMs. The meridional wind stress, however, does contribute to the strength of the cold season SST at the equator.

Presumably (although not demonstrated in the present model), the low-level cloud–radiation feedback would also enhance the cooperative feedback between the ECT and ITCZ (Mitchell and Wallace 1992). This has been demonstrated by Li (1997).

7. Conclusions and discussion

The annual march of ITCZ and associated mean climate asymmetry is a complex response of the coupled atmosphere–ocean–coastline system to solar radiation forcing. Critical elements determining the response include the land serving as an eastern ocean boundary, the antisymmetric insolation forcing (due to annual variation in the solar declination angle), the ITCZ–ECT interaction regulated by the antisymmetric solar forcing, and the annual variation of the symmetric insolation (due to annual variation of the earth–sun distance). The main points we would like to emphasize are summarized as follows.

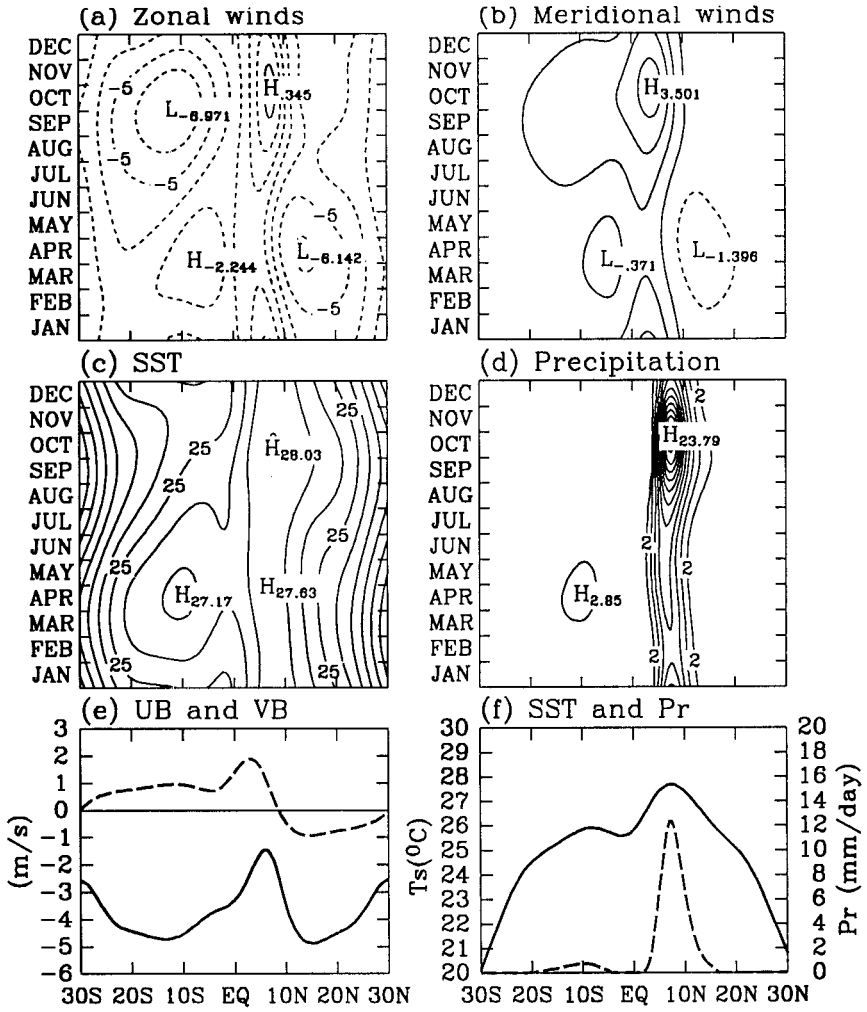

FIG. 11. The same as in Fig. 6 except that the effect of the tilted American coastline (the eastern boundary of the ocean) on ocean dynamics is included in the coupled model.

1) Without land effects, an aquaplanet mean climate of the coupled atmosphere–ocean system is symmetric with respect to the equator (Fig. 4), resembling that over the western Pacific warm pool (Fig. 2). Without an eastern boundary, the symmetric climate is stable to antisymmetric (monsoon) perturbations. Wind–evaporation feedback acts to damp antisymmetric perturbations and to maintain the symmetric climate.

2) It is the existence of land as an ocean *eastern boundary* that supports a finite-amplitude *east–west* SST gradient and associated easterlies and an ECT in the eastern ocean basin. The equatorial zonal asymmetry arises primarily from a balance between a coupled instability caused by SST gradient–zonal wind interaction and a stabilization caused by zonally differential surface buoyancy flux. The existence of the east–west asymmetry (or an ECT) is a necessary condition for creating a latitudinal climate asymmetry in the eastern Pacific and Atlantic Oceans.

3) The antisymmetric solar radiation forcing drives annual variation of the easterly trades, which in turn control annual variations of the ECT through changing upwelling. The annual cycle of the ECT is essentially a phase-delayed annual cycle of the ITCZ-free hemisphere. The interaction between the meridional SST gradient associated with the ECT and convection in the ITCZ provides a self-maintenance mechanism that prevents ITCZ following the sun and favors its stay in one hemisphere, either the NH or the SH depending on initial conditions. This bistable latitudinal climate asymmetry results from a delicate balance between the self-maintenance mechanism and the strength of antisymmetric insolation force (the period and amplitude of the variation in the solar declination angle). This mechanism relies on the mean stratification of the ocean (thermocline for instance) but does not rely on unstable coupled modes.

4) There are three key processes that ascertain the self-maintenance mechanism. (i) The delay of the annual cycle of the ECT with respect to the SST in the ITCZ-

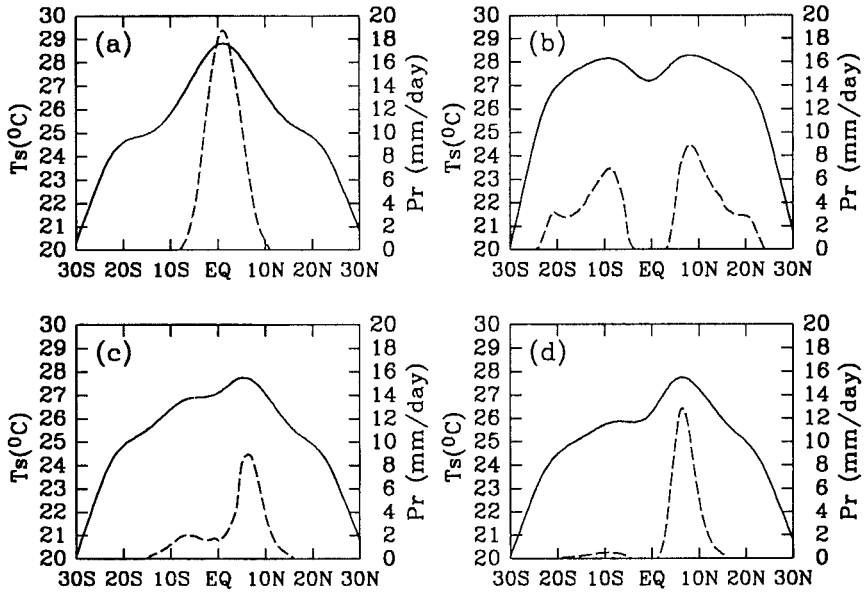

FIG. 12. Annual-mean SST (solid) and rainfall rate (dashed) simulated by the coupled model with annual cycle solar forcing and presence of the eastern ocean boundary in the experiments in which (a) the cooling associated with the equatorial upwelling is suppressed, (b) the wind-dependent evaporation is suppressed, (c) the SST gradient forcing on surface winds is suppressed, and (d) the meridional wind stress applied over the upper ocean is suppressed.

free hemisphere prolongs ITCZ's stay in the summer hemisphere. (ii) The meridional SST gradients between the ECT and ITCZ enhance moisture supply to the summer hemisphere ITCZ and sustain its strength there as long as the ECT remains. (iii) The off-equatorial heat source associated with the summer hemisphere ITCZ produces remarkable asymmetric Hadley circulation with winter hemisphere surface winds being much stronger, thus, the excessive evaporation cooling in the winter hemisphere delays and weakens the warming and ITCZ development there.

5) The annual variation of the solar radiation induced by the variation in the sun–earth distance favors the ECT to vary in phase with the annual cycle of the SH SST. This in-phase variation favors placement of warmest SST and ITCZ into the NH. Therefore, the annual cycle in the sun–earth distance can convert the bistable climate asymmetry into a preferred latitudinal asymmetry. The present-day sun–earth distance favors ITCZ staying in the NH.

6) With the annual-mean solar forcing, a northwest–southeast tilt of the eastern ocean boundary results in only a moderate preference of ITCZ in the NH (Philander et al. 1996). However, the antisymmetric solar forcing (due to the annual cycle in the solar declination angle) can substantially amplify the asymmetry via the mechanism described in (3) and (4) above.

Comparison of the mean climate asymmetry obtained in the experiments with and without the annual variation of insolation (Figs. 10a,b and 11e,f) clearly indicates the critical roles of the antisymmetric insolation forcing in the formation of the mean climate in the eastern Pacific and Atlantic Oceans. The antisymmetric insolation can act as either a contributor or a breaker to the latitudinal asymmetry, depending upon the competition between the ECT–ITCZ interaction and the antisymmetric solar forcing. The strength of the antisymmetric forcing varies with the period and maximum range of the variation in the solar declination angle. Sufficiently strong antisymmetric forcing (large amplitude or long periodicity) can, in principle, break latitudinal climate asymmetry, as demonstrated by Giese and Carton's (1994) GCM experiments. When the antisymmetric forcing cannot overcome the thermal inertia of the ocean and the resistance arising from the self-maintenance mechanism of the ITCZ–ECT complex, it contributes to generation of the latitudinal climate asymmetry by changing trade winds, by indirectly regulating annual variation of the ECT, and by initiating ITCZ–ECT interaction. It is important to recognize that the formation of the mean climate asymmetry is largely attributed to the annual cycle of the coupled system. Therefore, explanation of the mean climate formation without considering its annual variation or explanation of the annual variation by specifying a latitudinal asymmetric mean climate may lead to an incomplete physical picture.

The ITCZ–ECT interaction involves active ocean–atmosphere interaction. An effective ocean–atmosphere interaction requires significant changes in SST and convection be involved. Three processes may most efficiently change SST on large spatial scales: vertical advection associated with upwelling, downward solar radiation flux regulated by cloud amount, and surface latent heat flux. From an oceanographic point of view,

air–sea interactions associated with these processes should be potentially important. From an atmospheric point of view, the processes affecting convection and low-level moisture convergence contribute most to active air–sea interaction. Indeed, our sensitivity experiments indicate that the atmosphere–ocean interactions via changing the surface latent heat flux and moisture convergence are fundamental to the self-maintenance of latitudinal climate asymmetry. It should be pointed out that the stratus cloud decks are very effective at blocking solar radiation and changing SST, therefore, the cloud–radiation–SST feedback can be as effective as wind–evaporation feedback in promoting the self-maintenance mechanism.

The present model results indicate that both the variation of the earth–sun distance and the coastal forcing induced by a tilted eastern boundary are capable of selecting a preferred hemisphere. Because the model does not include cloud–radiation–SST feedback, it is unable to assess whether one is a more obvious candidate than the other in selecting the preferred latitudinal climate asymmetry. Other factors, such as hemispheric asymmetric distribution of land and ice coverage, can also serve as a symmetric climate breaker. But the annual cycle of solar forcing can further amplify the preferred latitudinal climate asymmetry as demonstrate in the present model. In view of the simplicity and limitations of the present theoretical model, some of the ideas and conclusions proposed in this study need to be tested using three-dimensional coupled models with more complete physics. This is under current investigation.

Acknowledgments. The authors would like to thank S. G. H. Philander, S.-P. Xie, W. Kessler, and G. Holland for their insightful comments. Two anonymous reviewers have provided thorough review and valuable comments, which helped improve the manuscript. Thanks are also extended to Mr. L. Wu and Mr. X. Fu for their assistance in processing data and preparing the manuscript. Support from the NOAA/PACS Program and ONR/Marine Meteorology Program under Grant 0014-95-1-1230 are greatly appreciated.

APPENDIX

Formulation of the Coupled Atmosphere–Ocean–Coastline Model

a. The atmospheric model

In the slab boundary layer, the zonal-mean winds, u_b and v_b are governed by

$$\frac{\partial u_b}{\partial t} + v_b\frac{\partial u_b}{\partial y} - \beta y v_b = -Eu_b, \tag{A.1a}$$

$$\frac{\partial v_b}{\partial t} + \beta y u_b = -Ev_b - \frac{\partial \phi}{\partial y} + A\frac{\partial T}{\partial y}, \tag{A.1b}$$

where A measures the boundary layer pressure gradient induced by SST gradients, which are proportional to the gas constant R and the depth of the boundary layer (Lindzen and Nigam 1987), E is a Rayleigh friction coefficient. The meridional advection of meridional momentum has been neglected in (A.1b), because it does not affect the solution appreciably.

The geopotential at the top of the boundary layer was assumed to equal the geopotential in the lower free troposphere. The free tropospheric motion stimulated by convective heating is described by the lowest baroclinic mode only (Gill 1980). The zonal-mean winds, u_a and v_a, and geopotential Φ in the lower free troposphere are governed by

$$\frac{\partial u_a}{\partial t} - \beta y v_a = -\epsilon_a u_a, \tag{A.2a}$$

$$\frac{\partial v_a}{\partial t} + \beta y u_a = -\epsilon_a v_a - \frac{\partial \Phi}{\partial y}, \tag{A.2b}$$

$$\frac{\partial \Phi}{\partial t} + C_a^2\left(\frac{\partial v_a}{\partial y} + d\frac{\partial v_b}{\partial y}\right) = -\frac{R\Delta p}{2C_p p_2}(Q_c + Q_r), \tag{A.2c}$$

where ϵ_a denotes the free atmosphere Rayleigh damping coefficient; C_a the dry atmospheric gravity wave speed of the lowest baroclinic mode; C_p the specific heat at constant pressure; Δp and p_2 the half-pressure depth of the free troposphere and the pressure at the middle of the free troposphere, respectively; $d = (p_s - p_e)/\Delta p$ is nondimensional boundary layer depth with p_s and p_e being the pressure at the surface and at the top of the boundary layer, respectively; Q_c and Q_r denote convective heating and longwave radiational cooling in the midtroposphere, respectively.

Following Davey and Gill (1987), the midtropospheric temperature perturbation is assumed to relax back, via longwave radiation, to an equilibrium temperature that has the same pattern as SST with a reduced variance. Thus

$$Q_r = \mu C_p\left[\frac{2p_2}{R\Delta p}\Phi + r(T - T_e)\right], \tag{A.3}$$

where μ is the reciprocal of the Newtonian cooling time; $2p_2/(R\Delta p)\Phi$ is the perturbation temperature at p_2; $(T - T_e)$ the deviation of SST from its domain mean $T_e = 298$ K; and r is the ratio of the temperature departure from the equilibrium temperature at p_2 to the SST deviation. The convective heating rate associated with precipitation rate P_r is

$$Q_c = \frac{gL_c}{\Delta p}\delta P_r, \tag{A.4}$$

where g and L_c are the gravity and latent heat, respectively, δ is a convection switch-on parameter, which depends on both the rainfall and SST (Wang and Li 1993);

$$\delta = \begin{cases} 1, & \text{if } T \geq 301 \text{ K and } P_r > 0, \\ (T_s - 299)/2, & \text{if } 299 < T < 301 \text{ K}, \\ & \quad \text{and } P_r > 0, \\ 0, & \text{otherwise.} \end{cases} \quad \text{(A.5)}$$

The precipitation rate P_r is determined by the boundary layer and lower free troposphere moisture convergence and surface evaporation E_v:

$$P_r = b\left[-\frac{\Delta p}{g}\left(q_a\frac{\partial v_a}{\partial y} + dq_b\frac{\partial v_b}{\partial y}\right) + E_v\right]. \quad \text{(A.6)}$$

Here we assumed that only a fraction, b, of the total moisture convergence condenses out, releasing latent heat. The mean specific humidity in the boundary layer and the lower free troposphere, q_b and q_a, is estimated by (Wang 1988)

$$q_b = q_0(p_s^m - p_e^m)/[m(p_s - p_e)], \quad \text{(A.6a)}$$

$$q_a = q_0(p_e^m - p_2^m)/[m(p_e - p_2)], \quad \text{(A.6b)}$$

where m is the ratio of the air density scale height (H = 7.8 km) and water vapor density scale height (H_w = 2.3 km); the surface air specific humidity is determined by SST via the following empirical formula (Li and Wang 1994):

$$q_0 = [0.972 \times T(°\text{C}) - 8.92] \times 10^{-3}. \quad \text{(A.7)}$$

The surface evaporation is calculated by

$$E_v = \rho_a C_E |V_B|[q_s(T) - q_0], \quad \text{(A.8)}$$

where ρ_a, C_E, $|V_B|$, and q_s are, respectively, the air density, turbulent heat transfer coefficient, surface wind speed, and saturation specific humidity at SST. When the time mean wind speed $|V_B| < 4$ m s^{-1}, E_v is calculated using a constant $|V_B| = 4$ m s^{-1} to account for transient wind effects on evaporation.

b. The ocean model

The mixed layer temperature T (or SST) zonally averaged in a longitudinally bounded basin is described by the mixed layer thermodynamic equation

$$\frac{\partial T}{\partial t} + v_s\frac{\partial T}{\partial y} + \frac{\partial v_s}{\partial y}\mathcal{H}\left(\frac{\partial v_s}{\partial y}\right)\Delta T_z = \frac{Q_{sw}(1-\gamma) - Q_{lw} - Q_{lh}}{\rho_w C_w H_s} - u_s\frac{\Delta T_x}{L_x} + \kappa\frac{\partial^2 T}{\partial y^2}, \quad \text{(A.9)}$$

where $\mathcal{H}$ represents the Heaviside function of x, u_s, and v_s the mixed layer zonal and meridional currents, ΔT_z is the difference between the SST and the temperature of the water upwelled into the mixed layer, ρ_w the water density, $C_w = 4.2 \times 10^3$ J Kg^{-1} K^{-1} the heat capacity of the water, H_s the depth of the mixed layer, and Q_{sw}, Q_{lw}, and Q_{lh} are, respectively, the downward heat flux at the sea surface due to shortwave radiation, longwave radiation, and evaporation, respectively; $\gamma = 0.1$ accounts for penetrated shortwave exiting through the bottom of the mixed layer; κ the turbulent diffusion coefficient. For simplicity, the heat fluxes are estimated by

$$Q_{sw} = F_0(1 - \alpha_A)(1 - 0.622C), \quad \text{(A.10a)}$$

$$Q_{lw} = \alpha(T - 273), \quad \text{(A.10b)}$$

$$Q_{lh} = L_c E_v, \quad \text{(A.10c)}$$

where α_A is albedo with a value of 0.08 used over the ocean, F_0 is shortwave radiation reaching the surface under clear sky, and C the total cloudiness, which is estimated, based on an observed total cloud fraction from the COADS as a function of latitude:

$$C = 0.44 + 0.27 \times \frac{|\phi|}{30°}. \quad \text{(A.11)}$$

Note that this distribution is symmetric about the equator so that the mean cloudiness does not create latitudinal climate asymmetry. The mixed layer currents can be written as sums of vertical mean currents, u_m and v_m, in the active upper ocean and the vertical shear, u_e and v_e, across the mixed layer base:

$$(u_s, v_s) = \left(u_m + u_e\frac{H - H_s}{H}, v_m + v_e\frac{H - H_s}{H}\right). \quad \text{(A.12)}$$

The u_m and v_m are governed by zonally averaged upper-ocean dynamical equations:

$$\frac{\partial u_m}{\partial t} - \beta y v_m = -\epsilon_o u_m + \frac{\tau_x}{\rho_w H}, \quad \text{(A.13a)}$$

$$\frac{\partial v_m}{\partial t} + \beta y u_m = -\epsilon_o v_m + \frac{\tau_y}{\rho_w H} - g'\frac{\partial h}{\partial y}, \quad \text{(A.13b)}$$

$$\frac{\partial h}{\partial t} + H\frac{\partial v_m}{\partial y} = -\epsilon_o h + \kappa\frac{\partial^2 h}{\partial y^2}, \quad \text{(A.13c)}$$

where H is the mean thermocline depth, g' the reduced gravity, ϵ_o the Rayleigh damping coefficient in the upper ocean, and the wind stresses are estimated from the bulk formula

$$(\tau_x, \tau_y) = \rho_a C_D |V_B|(u_B, v_B). \quad \text{(A.14)}$$

The vertical shears u_e and v_e can be solved from the steady mixed layer Ekman dynamics:

$$r_s u_e - \beta y v_e = \frac{\tau_x}{\rho_w H}, \quad \text{(A.15a)}$$

$$r_s v_e + \beta y u_e = \frac{\tau_y}{\rho_w H}. \quad \text{(A.15b)}$$

REFERENCES

Battisti, D. S., and A. C. Hirst, 1989: Interannual variability in the tropical atmosphere–ocean system: Influence of the basic state and ocean geometry. *J. Atmos. Sci.,* **46,** 1678–1712.

Bjerknes, 1969: Atmospheric teleconnection from the equatorial pacific. *Mon. Wea. Rev.,* **97,** 526–535.

Budyko, M. I., and D. H. Miller, 1974: *Climate and Life.* Academic Press, 508 pp.

Chang, P., 1996: The role of the dynamic ocean–atmosphere interactions in the tropical seasonal cycle. *J. Climate,* **9,** 2973–2985.

——, and S. G. H. Philander, 1994: A coupled ocean–atmosphere instability of relevance to seasonal cycle. *J. Atmos. Sci.,* **51,** 3627–3648.

Charney, J. G., 1971: Tropical cyclogenesis and the formation of the intertropical convergence zone. *Mathematical Problems of Geophysical Fluid Dynamics,* W. H. Reid, Ed., *Lectures in Applied Mathematics,* Vol. 13, Amer. Math. Soc., 355–368.

Davey, M. K., and Gill, A. E., 1987: Experiments on tropical circulation with a simple moist model. *Quart. J. Roy. Meteor. Soc.,* **113,** 1237–1269.

Dijkstra, H. A., and J. D. Neelin, 1995: Ocean–atmospheric interaction and the tropical climatology. Part II: Why the Pacific cold tongue is in the east. *J. Climate,* **8,** 1343–1359.

Giese, B. S., and J. A. Carton, 1994: The seasonal cycle in a coupled ocean–atmosphere model. *J. Climate,* **7,** 1208–1217.

Gill, A. E., 1980: Some simple solutions for heat-induced tropical circulation. *Quart. J. Roy. Meteor. Soc.,* **106,** 447–462.

Held, I. M., and A. Y. Hou, 1980: Nonlinear axially symmetric circulations in a nearly inviscid atmosphere. *J. Atmos. Sci.,* **37,** 515–533.

Holton, J. R., J. M. Wallace, and J. A. Young, 1971: On boundary layer dynamics and the ITCZ. *J. Atmos. Sci.,* **28,** 275–180.

Horel, J. D., 1982: On the annual cycle of the tropical Pacific atmosphere and ocean. *Mon. Wea. Rev.,* **110,** 1863–1878.

Jin, F.-F., 1996: Tropical ocean–atmosphere interaction, the Pacific cold tongue, and the El Nino–Southern Oscillation. *Science,* **274,** 76–78.

Li, T., 1997: Air–sea interaction of relevance to the ITCZ: Analysis of coupled instability and experiments in a hybrid coupled GCM. *J. Atmos. Sci.,* **54,** 134–147.

——, and B. Wang, 1994: A thermodynamic equilibrium climate model for monthly mean surface winds and precipitation over the tropical Pacific. *J. Atmos. Sci.,* **51,** 1372–1385.

Lindzen, R. S., and S. Nigam, 1987: On the role of sea surface temperature gradients in forcing low level winds and convergence in the tropics. *J. Atmos. Sci.,* **44,** 2440–2458.

——, and A. Y. Hou, 1988: Hadley circulations for zonally averaged heating centered off the equator. *J. Atmos. Sci.,* **45,** 2416–2427.

Liu, Z., and S.-P. Xie, 1994: Equatorward propagation of coupled air–sea disturbances with application to the annual cycle of the eastern tropical Pacific. *J. Atmos. Sci.,* **51,** 3807–3822.

Ma, C.-C., C. R. Mechoso, A. W. Robertson, and A. Arakawa, 1996: Peruvian stratus clouds and the tropical Pacific circulation: A coupled ocean–atmosphere GCM study. *J. Climate,* **9,** 1635–1645.

Mitchell, T. P., and J. M. Wallace, 1992: On the annual cycle in equatorial convection and sea surface temperature. *J. Climate,* **5,** 1140–1152.

Murakami, T., B. Wang, and S. W. Lyons, 1992: Summer monsoon over the Bay of Bengal and the eastern North Pacific. *J. Meteor. Soc. Japan,* **70,** 191–210.

Nigam, S., and Y. Chao, 1996: Evolution dynamics of tropical ocean–atmosphere annual cycle variability. *J. Climate,* **9,** 3187–3205.

O'Brien, J. J., and H. E. Hurlburt, 1972: A numerical model of coastal upwelling. *J. Phys. Oceanogr.,* **2,** 14–26.

Philander, G., D. Gu, D. Halpern, G. Lambert, N.-C. Lau, T. Li, and R. C. Pacanowski, 1996: Why the ITCZ is mostly north of the equator. *J. Climate,* **9,** 2958–2972.

Sadler, J. C., M. A. Lander, A. M. Hori, and K. Oda, 1987: *Pacific Ocean.* Vol. 1. *Tropical Marine Climate Atlas.* Rep. UHMET 87-02, Department of Meteorology, University of Hawaii, 27 pp.

Sverdrup, H., 1947: Wind-driven currents in a baroclinic ocean, with application to the equatorial currents of the eastern Pacific. *Natl. Acad. Sci.,* **33,** 318–326.

Waliser, D. E., and R. C. J. Somerville, 1994: Preferred latitudes of the intertropical convergence zone. *J. Atmos. Sci.,* **51,** 1619–1639.

Wang, B., 1988: Dynamics of tropical low-frequency waves: An analysis of the moist Kelvin wave. *J. Atmos. Sci.,* **45,** 2051–2065.

——, 1994: On the annual cycle in the eastern-central Pacific. *J. Climate,* **7,** 1926–1942.

——, and T. Li, 1993: A simple tropical atmosphere model of relevance to short-term climate variations. *J. Atmos. Sci.,* **50,** 260–284.

——, and ——, 1994: Convective interaction with boundary layer dynamics in the development of a tropical intraseasonal system. *J. Atmos. Sci.,* **51,** 1386–1400.

——, and Z. Fang, 1996: Chaotic oscillation of the tropical climate: A dynamic system theory for ENSO. *J. Atmos. Sci.,* **53,** 2786–2802.

Xie., P., and P. Arkin, 1996: Analysis of global monthly precipitation using gauge observations, satellite estimates, and numerical model predictions. *J. Climate,* **9,** 840–858.

Xie, S.-P., 1996: Westward propagation of latitudinal asymmetry in a coupled ocean–atmosphere model. *J. Atmos. Sci.,* **53,** 3236–3250.

——, 1997: Unstable transition of the tropical climate to an equatorially asymmetric state in a coupled ocean–atmosphere model. *Mon. Wea. Rev.,* **125,** 667–679.

——, and S. G. H. Philander, 1994: A coupled ocean–atmosphere model of relevance to the ITCZ in the eastern Pacific. *Tellus,* **46A,** 340–350.

Zebiak, S. E., and M. A. Cane, 1987: A model ENSO. *Mon. Wea. Rev.,* **115,** 2262–2278.